PAGEOPH, Vol. 147, No. 4 (1996)

0033-4553/96/040789-31$1.50 + 0.20/0

Numerical Simulation of a Mesolow over a Gulf Stream Filament

SETHU RAMAN[1] and NEERAJA C. REDDY[1]

Abstract – A three-dimensional mesoscale numerical model is used to investigate mesoscale circulation over a Gulf Stream filament. Two numerical experiments are performed with different initial uniform ambient wind speeds ($U = 0.1$ m s^{-1}, 3.5 m s^{-1} and 7 m s^{-1}) for a typical winter day. It is found that for both low and moderate winds, a closed mesoscale circulation forms over the Gulf Stream filament. When the Gulf Stream filament was removed, the model did not predict a mesoscale circulation. The modeled circulation over the filament is in agreement with the observations, suggesting that the atmospheric circulations over the filaments may be an important mechanism in the U.S. East Coast cyclogenesis.

Key words: Gulf Stream, mesoscale, East Coast cyclogenesis.

1. Introduction

Cyclogenesis can result from a variety of distinct or cooperative dynamic mechanisms and complex scale interactions. Existence of a spatial maxima in the global distribution of cyclogenesis frequency points to the importance of local forcing (PETTERSSEN, 1956). The local factors include mountain ranges, coastal regions and sea-surface temperature (SST) contrasts. Often two or more of these effects act in concert along the East Coast of the United States. An important ingredient of the winter cyclogenesis is the formation of a mesoscale coastal front.

Presence of the Gulf Stream is another major factor in the East Coast cyclogenesis. The climatologies of cyclones show distinct frequency maxima near the Atlantic coastline or over the Gulf Stream. For example, SANDERS and GYAKUM's (1980) dynamic climatology of explosive cyclogenesis identifies the Gulf Stream as a preferred area for rapid development. However, even though it is generally acknowledged that the thermodynamic forcing by the Gulf Stream is an important factor in U.S. East Coast frontogenesis and cyclogenesis, until

[1] North Carolina State University, Raleigh, NC 27695-8208, U.S.A.

recently no effort has been made to understand the role of the Gulf Stream meandering.

Many investigators have shown that the Gulf Stream meanders appreciably due to its own dynamics (PIETRAFESA, 1978; ROONEY *et al.*, 1978). A topographic feature on the upper slope of the Atlantic Ocean bottom located near 32 N, 79 W known as the "Charleston bump" causes an eastward deflection of the Gulf Stream, resulting in a quasi-permanent excursion of the Gulf Stream front downstream. A frequently observed feature related to the Gulf Stream meandering in this region is the warm-core folded back filaments or shingles (VON ARX *et al.*, 1955). The southward oriented shingles are long tongue-like extrusions of the Gulf Stream surface waters onto the shelf. PIETRAFESA (1983) showed that the frequency of these events is between 2–12 per month on the North Carolina shelf during winters. Typical length and width of these Gulf Stream filaments are observed to be 200 km and 50 km, respectively.

REDDY and RAMAN (1994) documented the formation of a mesolow over a Gulf Stream filament for 10 February 1986 by using the data collected during the Genesis of Atlantic Lows Experiment (GALE) IOP # 5. This mesolow formed in conjunction with a shallow mesoscale front aligned along the eastern edge of the Gulf Stream. CIONE *et al.* (1993) showed that nearer the Gulf Stream to the coastline, more frequently do the East Coast storms develop or intensify because of the increased boundary layer baroclinicity. The formation of the Gulf Stream filaments tends to decrease the distance between the western edge of the Gulf Stream and the coastline.

Numerical studies of the marine boundary layer in this region have been conducted by many investigators (BROST, 1976; MOENG and ARAKAWA, 1980; ATLAS *et al.*, 1983; WAI and STAGE, 1989; WARNER *et al.*, 1990; HUANG and RAMAN, 1992). In the simulations of the marine boundary layer induced by a single Gulf Stream front, WAI and STAGE (1989) showed that a convective boundary layer forms offshore and slopes up seawards in response to the increasing modification of the low-level air. Earlier stages of the development of mesoscale circulation induced by steady ocean warming are somewhat similar to those of sea breeze circulations (MAHRER and PIELKE, 1977, 1978).

Although several numerical studies have been conducted on the modification of the marine boundary layer by many investigators, none investigated the importance of Gulf Stream meandering and its associated filaments on coastal cyclogenesis. Our previous observational study (REDDY and RAMAN, 1994) was the main impetus for this numerical investigation. A three-dimensional numerical model developed by HUANG and RAMAN (1990, 1992) is used. A brief description of the numerical model is presented in Section 3. Numerical schemes and the initial and boundary conditions used in the model are described in Section 4. Results from the numerical experiments that pertain to the mesoscale circula-

tions, structure of the marine boundary layer, the geometry of oceanic rainbands and the role of the Gulf Stream filaments are discussed in Section 5.

2. Synoptic and Mesoscale Conditions

A high pressure system dominated the East Coast of the United States at 12 UTC on 9 February 1986, causing northerly winds offshore (Fig. 1a). In the GALE region (region offshore of Carolinas, 30–37 N, 70–80 W), gradual veering of the offshore winds from north-northeasterly to east-northeasterly accompanied the eastward shift of the anticyclone. Over land (East Coast of the U.S.), however, the wind direction remained northeasterly as a ridge of high pressure extended southwestward along the coast, east of the Appalachian Mountains. At 12 UTC (Fig. 1c) on 10 February, a mid-tropospheric trough extended southwest, with the northern tip of the trough located offshore of North Carolina and the southern tip of the trough located near the South Carolina coast. A low pressure system developed offshore of North Carolina. From 12 UTC to 21 UTC (Figs. 1c, 1d and 1e) on 10 February, a stationary front was located off the coast almost parallel to the Gulf Stream. Aircraft observations taken during this period indicated a mesoscale circulation which may be associated with a mesolow over the Gulf Stream region (Fig. 2). This mid-tropospheric trough migrated offshore by 12 UTC on 11 February (Fig. 1f). This trough is believed to have caused the intensification of the mesolow.

The mesoscale analysis at 17 UTC, 10 February, is shown in Figure 2. The streamline analysis (Fig. 2a) indicated two confluence zones (heavy solid lines) and a diffluence zone in between. The winds increased by a factor of two from $4.8\ m\ s^{-1}$ over the mid-shelf waters to $9.5\ m\ s^{-1}$ at the western edge of the Gulf Stream. Existence of a mesolow is evident in Figure 2a. The contours of computed horizontal divergence, shown in Figure 2b, indicate two low-level mesoscale convergence zones, one near the western edge of the Gulf Stream ($7.8 \times 10^{-5}\ s^{-1}$, heavy solid line) and the other near the coastal waters offshore of Wilmington ($3.4 \times 10^{-5}\ s^{-1}$, heavy solid line) with a divergence zone in between ($3.1 \times 10^{-5}\ s^{-1}$, heavy dashed line). Similar convergence/divergence zones were also observed by RIORDAN (1990) and HOLT and RAMAN (1990) for other days during coastal frontogenesis. Mesoscale analysis on 11 February indicated a northwesterly flow near the coast and southwesterly flow over the western Atlantic. The wind speeds increased offshore due to the deepening of the surface mesolow as a mid-tropospheric trough moved into the region.

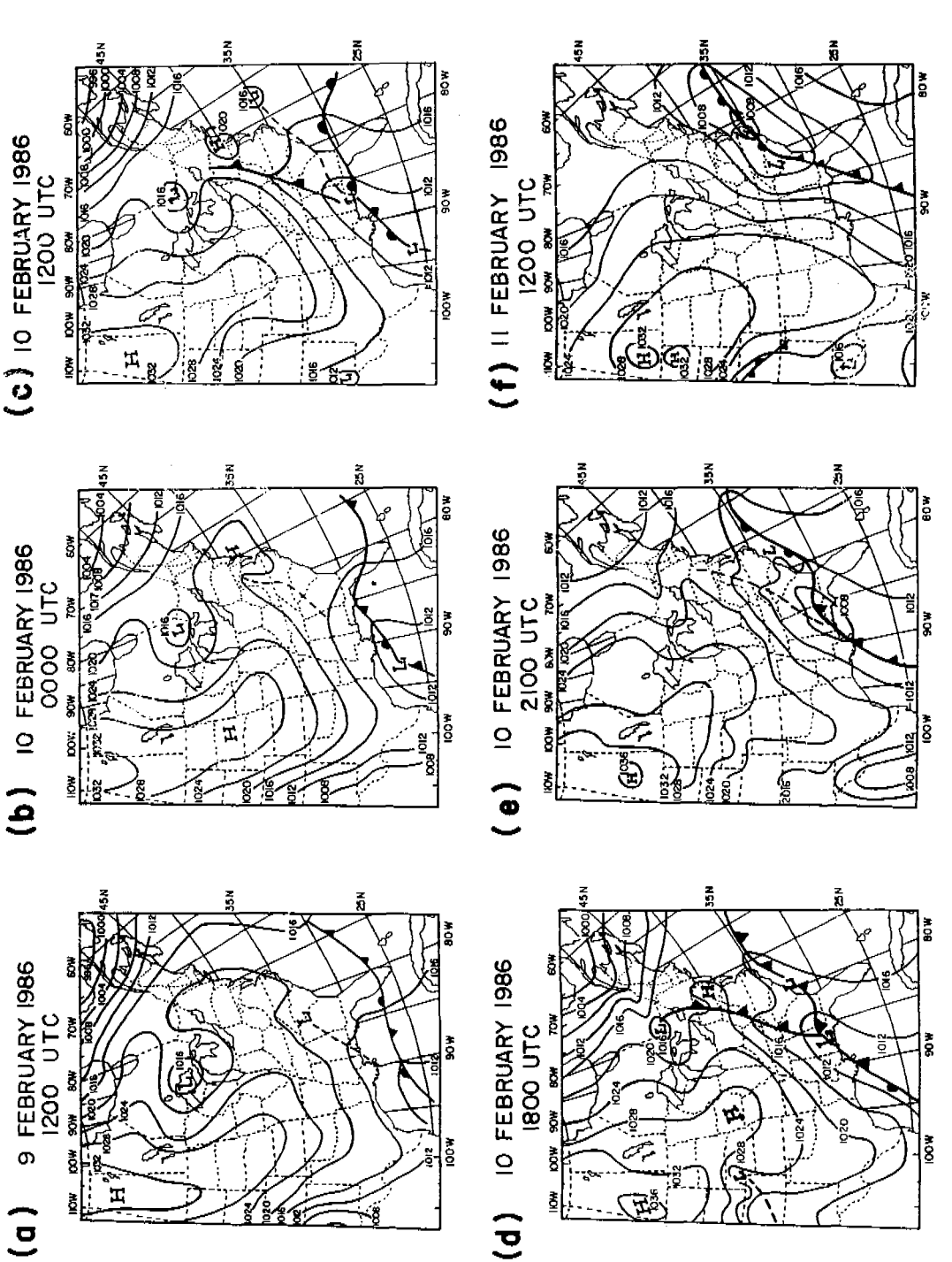
(a) 9 FEBRUARY 1986 1200 UTC
(b) 10 FEBRUARY 1986 0000 UTC
(c) 10 FEBRUARY 1986 1200 UTC
(d) 10 FEBRUARY 1986 1800 UTC
(e) 10 FEBRUARY 1986 2100 UTC
(f) 11 FEBRUARY 1986 1200 UTC

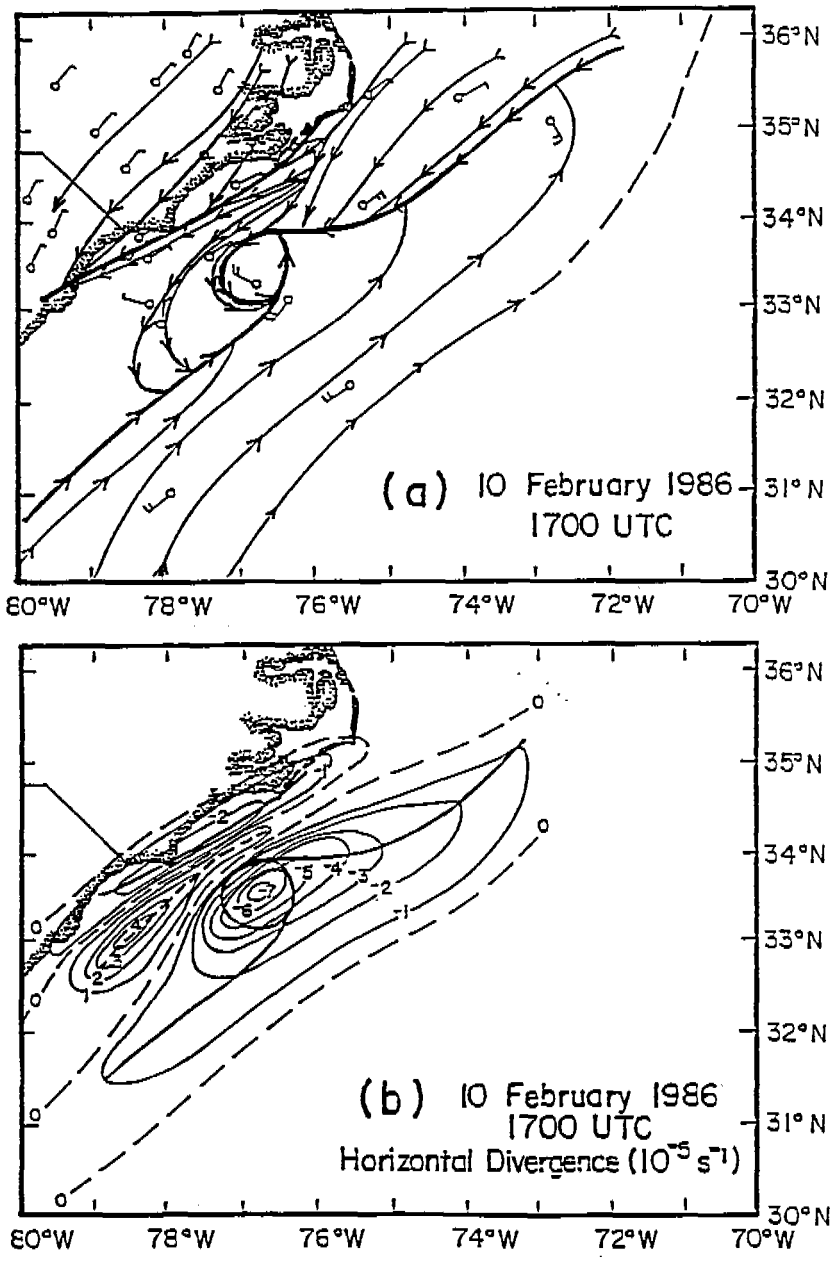

Figure 2
Mesoscale analysis on 10 February at 1700 UTC, (a) streamline analysis and (b) horizontal divergence.

Figure 1
Synoptic analysis on (a) 9 February at 1200 UTC, (b) 10 February at 0000 UTC, (c) 10 February 1200 UTC, (d) 10 February 1800 UTC, (e) 10 February 2100 UTC and (f) 11 February 1200 UTC.

3. Model Description

The three-dimensional mesoscale numerical model used in this study is described by HUANG and RAMAN (1988, 1991). A domain height of 8 km is used in the model for all simulations. The model is hydrostatic and anelastic in a terrain following coordinate system. The prognostic model equations include the horizontal momentum equations, the thermodynamic equation for the potential temperature, and the conservation equations for water vapor q, cloud water q_c and rainwater q_r.

The atmospheric planetary boundary layer is treated separately as the surface layer and a transition layer in the model. To account for the surface layer turbulent transport, the surface-layer similarity stability functions given by BUSINGER *et al.* (1971) are used. Above the surface layer, a turbulence closure scheme using the turbulent kinetic energy (TKE) and dissipation (ε) is incorporated with the level 2.5 scheme of MELLOR and YAMADA (1982) to determine the eddy diffusivities in the transition layer.

The ground temperature is obtained from the surface energy balance equation, while the sea-surface termperature is held constant. The radiation scheme used in this model incorporates long-wave and short-wave radiation transfer which is similar to the one used by MAHRER and PIELKE (1977). This scheme takes into account the absorption of short-wave radiation by water vapor and long-wave energy emitted by the water vapor and carbon dioxide. A variation of Kuo's scheme (KUO, 1974) is incorporated to account for the subgrid-scale cloud effects that cannot be resolved by the grid points. Subgrid shallow clouds are not considered in this study.

To account for advection effects, an improved form of the Crowley type advection scheme, termed the modified upstream scheme or Warming-Kutler-Lomax (WKL) advection scheme (WARMING *et al.*, 1973; HUANG and RAMAN, 1990) is used in the horizontal and a quadratic upstream interpolation in the vertical. In order to obtain initial conditions, an Ekman-layer type balance equation is applied to determine an initial velocity profile, while the potential temperature and relative humidity profiles are specified at the initial time. At the lower boundary, a no-slip condition is imposed for the wind. The relative humidity near the ground is held constant. The hydrostatic equation is used to obtain the surface pressure with known upper level pressure. At the upper boundary, a radiation boundary condition (KLEMP and DURRAN, 1983) is used to determine the perturbation pressure. A prognostic scheme (MILLER and THORPE, 1981) is applied at the lateral inflow boundary grids while prediction equations are used at the lateral outflow boundary.

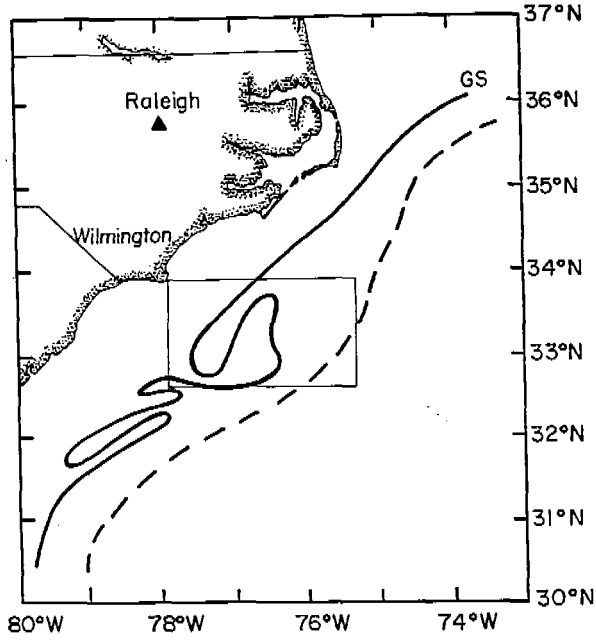

Figure 3
Model domain overlaid the Gulf Stream and the filament.

4. Experiment Design

The Gulf Stream position was obtained from a report provided by the NOAA/AOML (Atlantic Oceangraphic and Meteorological Laboratories) at 1800 UTC on 10 February, 1986 and is shown in Figure 3. The solid line corresponds to the maximum SST contour of 25°C, indicating the western edge of the Gulf Stream. The eastern edge of the Gulf Stream is indicated by the dashed contour line of 23°C. As can be seen from Figure 3, three filaments formed on 10 February. The King Air aircraft took observations across the filament on 10 February. The detailed analyses and results are given in REDDY and RAMAN (1994). The observations indicated weak northeasterly winds of about 3–4 m s^{-1}.

Table 1

Numerical experiments

Case	Filament	Wind speed (m s^{-1})	Wind dir.	SST	Model resolution
C1	YES	3.5	NE	Constant SST	4 km
C2	YES	0.1	NE	Constant SST	4 km
C3	NO	3.5	NE	Constant SST	4 km
C4	YES	3.5	NE	Realistic SST	4 km

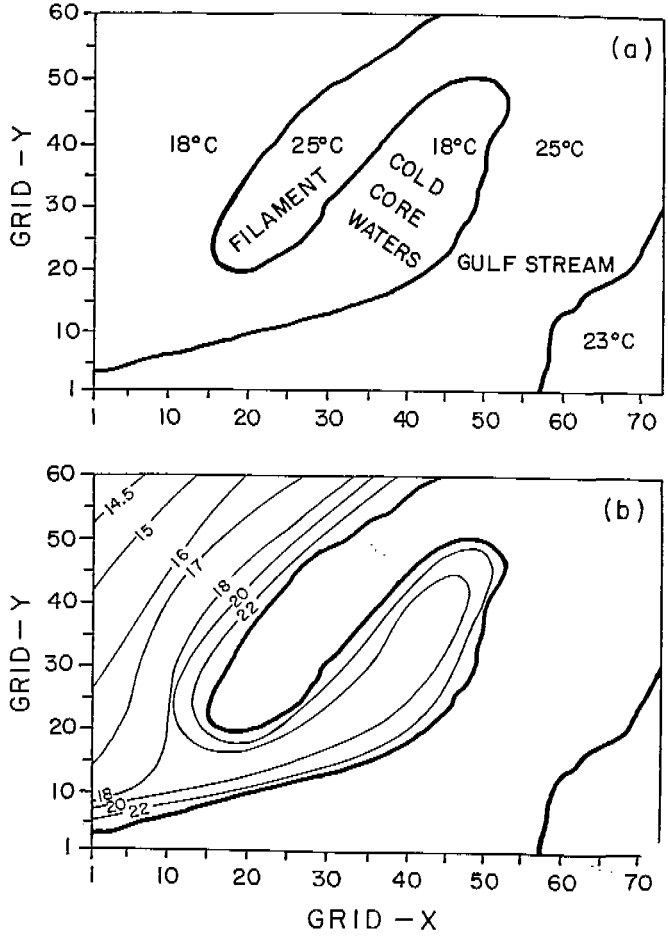

Figure 4
SST distribution in the model domain, (a) for experiments C1 - C3 and (b) for experiment C4.

The model domain for the numerical experiments C1–C4 is indicated by the rectangular box (Fig. 3). Descriptions of the experiments are given in Table 1. An enlarged version of the rectangular box, along with the sea-surface temperature distribution used for these experiments, is shown in Figure 4. In the vertical, 15 stretched grid points are used for all the experiments with a domain height of 8 km. The model has a higher vertical resolution at lower levels (see Table 2). The horizontal model domain covers 73 grid points in the x direction and 60 grid points in the y direction with a uniform grid spacing of 4 km. SST distribution observed on 10 February 1986 is used for the case C4 simulation (Fig. 4b).

Table 2

Model levels

Model layer	Height (m)
1	50
2	150
3	250
4	500
5	750
6	1000
7	1500
8	2000
9	2500
10	3000
11	4000
12	5000
13	6000
14	7000
15	8000

Barotropic ambient conditions are used for all simulations, with a constant vertical potential temperature gradient of $4\,C\,km^{-1}$. Moisture conditions for the domain are prescribed by a profile with 80% relative humidity below 1 km. Above this height, the relative humidity is assumed to decrease linearly to zero at 5 km. Barotropic conditions are assumed initially. Magnitudes of the wind speeds for different cases are given in Table 1.

Initialization of the mesoscale model is based on prescribed 1D profiles and a solution of the Ekman-gradient wind equations. The cases C1 (ambient wind $3.5\,m\,s^{-1}$) and C2 (weak ambient winds) are conducted to investigate the dependence of the intensity of circulation on ambient winds. Case C3 is conducted to investigate the influence of the filament on the development and intensification of offshore mesolows. Case C4, is similar to Case C1 except that realistic SST distribution is used. All cases are integrated for 15 h.

5. *Model Results*

An initial uniform wind speed of $3.5\,m\,s^{-1}$ is used in case C1 to investigate the mesoscale circulation observed on 10 February 1986 over a Gulf Stream filament. Case C2 is simulated with weak initial uniform wind speed. Initial conditions used for cases C3 and C4 are the same as those for case C1 except that case C3 is simulated without a Gulf Stream filament and case C4 is simulated with a realistic SST distribution (see Fig. 4b).

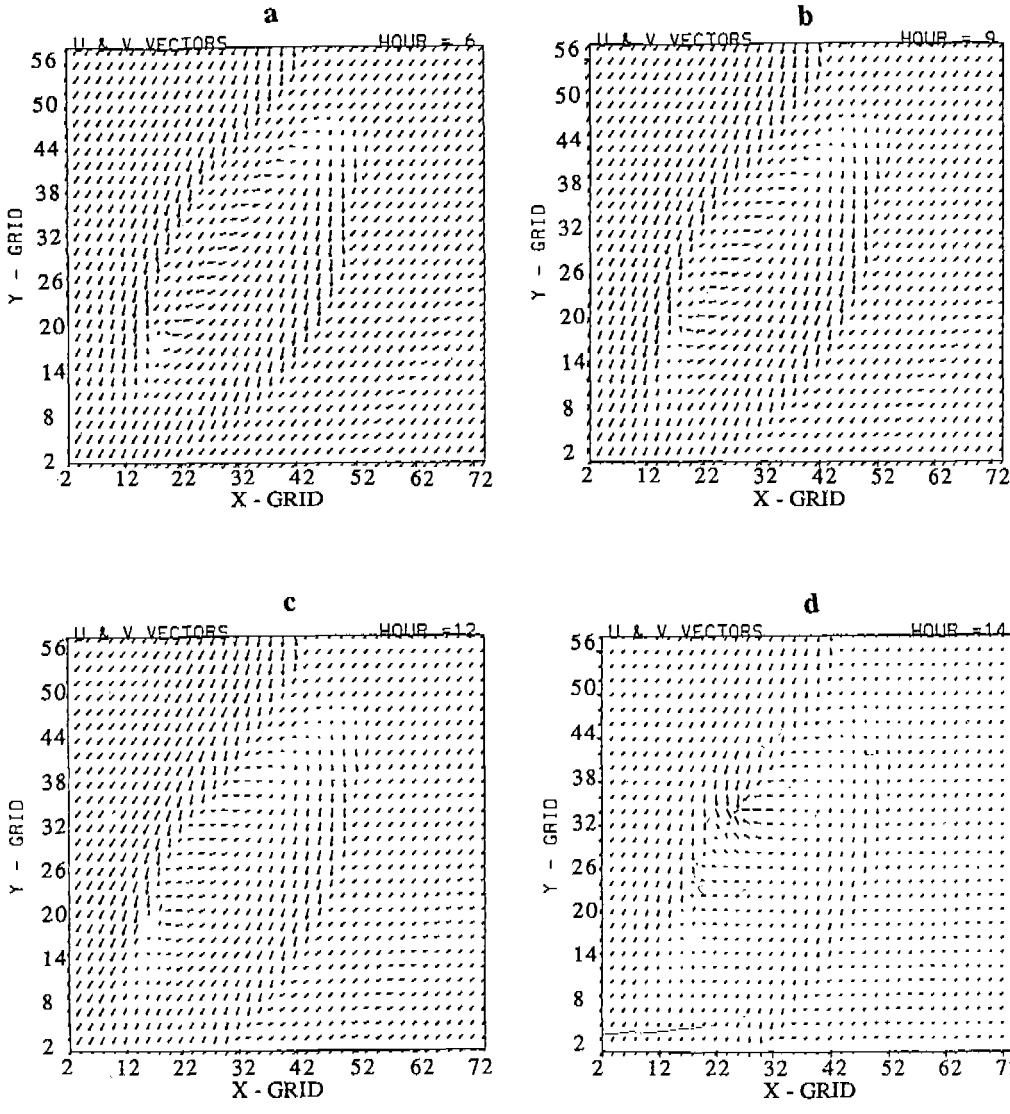

Figure 5
Spatial distribution of U and V vectors at (a) 6 h, (b) 9 h, (c) 12 h and (e) 15 h of model simulation for case C1 at 50 m height. The maximum wind speeds are respectively 5.0 m s $^{-1}$, 6.1 m s^{-1}, 9.5 m s^{-1} and 12.5 m s $^{-1}$ at these hours.

5.1 Sensitivity to Different Ambient Winds

(a) Moderate Ambient Wind (Case C1 with a wind speed of 3.5 m s^{-1})

Figure 5 displays the U and V vectors after 6 h, 9 h, 12 h and 14 h of simulation at a height of 50 m (layer 2). The predicted wind distribution at the initial stages

(Fig. 5a) of simulation indicates a weak convergence zone along the edges of the maximum SST contour. However, the convergence at the edges of the filament is much stronger as compared to the one along the western edge of the Gulf Stream. A divergence zone exists between the filament and the western edge of the Gulf Stream. The flow west of the convergence zone turns southwards as it responds to locally generated pressure gradients due to differential surface heating. Similarly, the flow east turns northward. In response to the frontogenetical flow, the

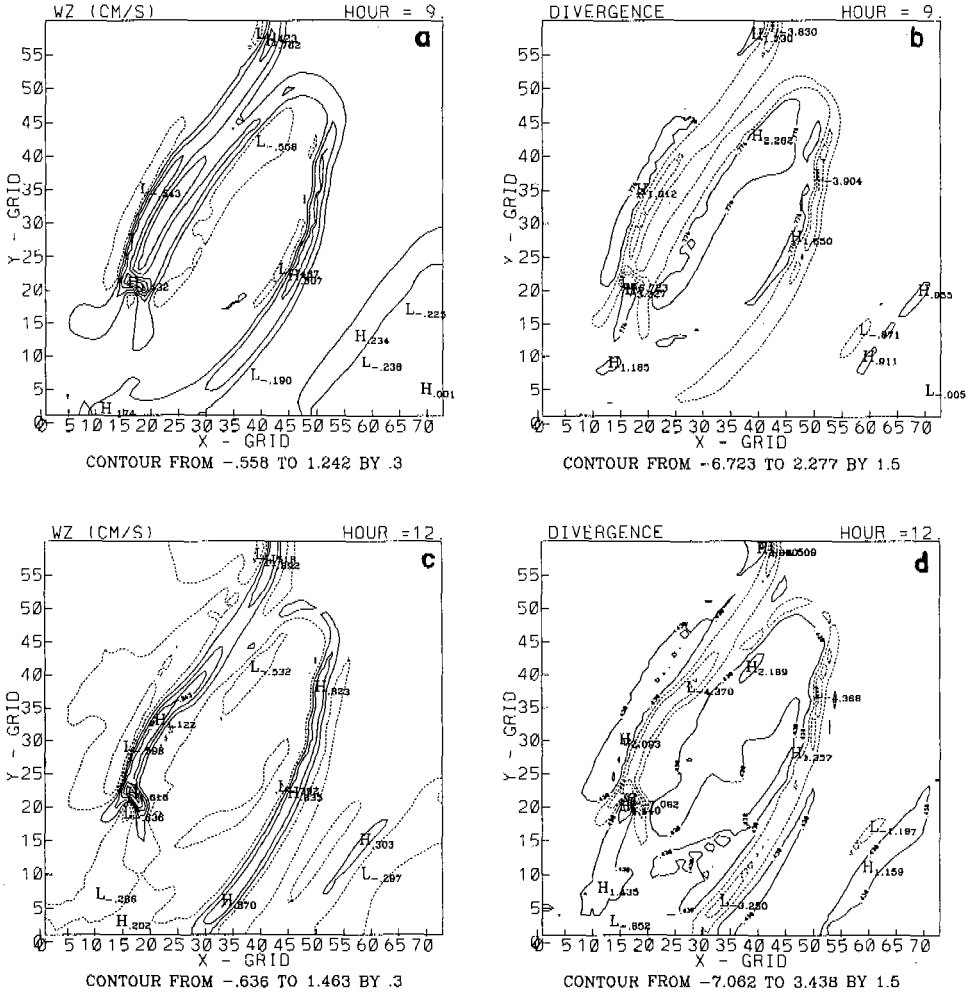

Figure 6
Spatial distribution of (a) vertical velocity in cm s $^{-1}$ at 9 h, (b) horizontal divergence ($\times 10^{-5}$) at 9 h, (c) vertical velocity in cm s^{-1} at 12 h, (d) horizontal divergence ($\times 10^{-5}$) at 12 h of model simulation at 50 m for case C1.

mesoscale circulation becomes more discernible after 9 h (Fig. 5b) of integration. The flow pattern with a cyclonic wind shift line is favorable for maximizing the coastal frontogenesis, since the line (acting as an axis of dilatation) is almost along an isotherm (PETTERSEN, 1956). After 12 h of integration (Fig. 5c), the wind vectors turned cyclonically over the filament, indicating the development of a mesolow over this region. This mesolow further intensified into a close mesoscale circulation at 14 h (Fig. 5d).

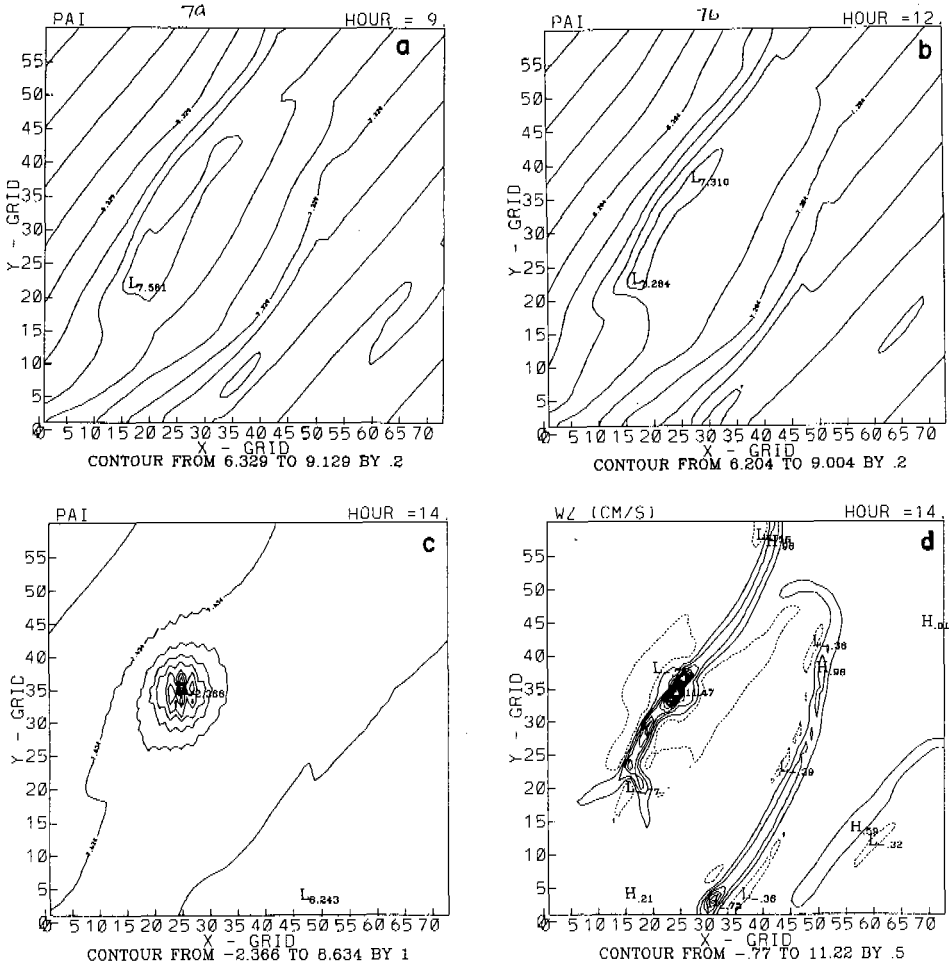

Figure 7
Spatial distribution of (a,b,c) surface pressures (mb) at (a) 9 h, (b) 12 h, and (c) 15 h and (d) vertical velocities (cm s^{-1}) at 50 m height for Case C1 at 15 h of simulation.

It will be of interest to compare the model predicted horizontal divergences and wind speeds with the observations (Fig. 2). The contours of horizontal divergences and vertical veolcities after 9 h and 12 h of integration are shown in Figure 6. As expected, the model predicted convergence values are maximum over the filament, with small values over the Gulf Stream. The predicted maximum divergence values are $-6.7 \times 10^{-5}\,s^{-1}$ to $3.3 \times 10^{-5}\,s^{-1}$ after 9 h (1800 UTC) and $-7.1 \times 10^{-5}\,s^{-1}$ and $4.4 \times 10^{-5}\,s^{-1}$ after 12 h (2100 UTC) of integration (Figs. 6a and 6b), respectively. The observed maximum horizontal divergence values (Fig. 2b) were about $-7.1 \times 10^{-5}\,s^{-1}$ and $4.2 \times 10^{-5}\,s^{-1}$ at 1700 UTC. It is encouraging to find that the predicted values are of the same order of magnitude as the observations.

Maximum ascending motion is predicted along the edges of the filament. The maximum ascent at 50 m increased from $1.14\,cm\,s^{-1}$ after 6 h of integration to $11.5\,cm\,s^{-1}$ (Figs. 6c, 6d and 7d) at 14 h. The maximum vertical velocities in the model after 9 h and 12 h are $2.0\,cm\,s^{-1}$ and $3.5\,cm\,s^{-1}$, respectively. Relatively weaker vertical motions occur along the Gulf Stream (Fig. 7d) with a magnitude of $2.87\,cm\,s^{-1}$ after 14 h of model simulation. The contours of surface pressures shown in Figure 7 (surface pressure p minus 1000 mb) indicate a decreasing trend over the filament with a low pressure of 1004 mb at 6 h. Pressure at this location decreases to 998 mb at 14 h of integration. During the initial stages of the model run (after 6 h), circulation starts developing over the filament and intensifies into a mesolow as time progresses. The wind speeds increase from an initial value of $3.5\,m\,s^{-1}$ to $13.0\,m\,s^{-1}$ at 14 h of model simulation (Fig. 5) over the Gulf Stream filament. The observed wind speeds over the Gulf Stream filament were about $12\,m\,s^{-1}$.

The distribution of sensible and latent heat fluxes after 9 h and 12 h of model integration are shown in Figure 8. The contours indicate a maximum value over the Gulf Stream filament. The predicted maximum values of total heat fluxes (sensible heat flux + latent heat flux) are about $200\,Wm^{-2}$ and $250\,Wm^{-2}$, respectively over the Gulf Stream filament after 9 h and 12 h of model integration. A total heat flux of $240\,Wm^{-2}$ was observed over a Gulf Stream filament on 10 February (REDDY and RAMAN, 1994). The contours of latent heat fluxes show sharp gradients west of the filament.

To better understand the vertical structure of the flow over the filament, a cross section of the contours of potential temperature (θ), turbulence kinetic energy (TKE), wind speed and U-W vectors is examined ($Y = 25$) at 9 h across a region of strong convection located at the edges of the filament (Fig. 9). This cross section is in a vertical plane (x-z) from west to east. The horizontal gradient of potential temperature manifests a well-defined sea-breeze type of circulation over the filament after 12 h of simulation. This circulation is shallow and extends to a height of about 1600 m (Figs. 9 and 10). As can be seen from the figure, there is a strong convergence at the edges of the filament. Observations in this region indicated a shallow circulation extending up to 1 km (REDDY and RAMAN, 1994).

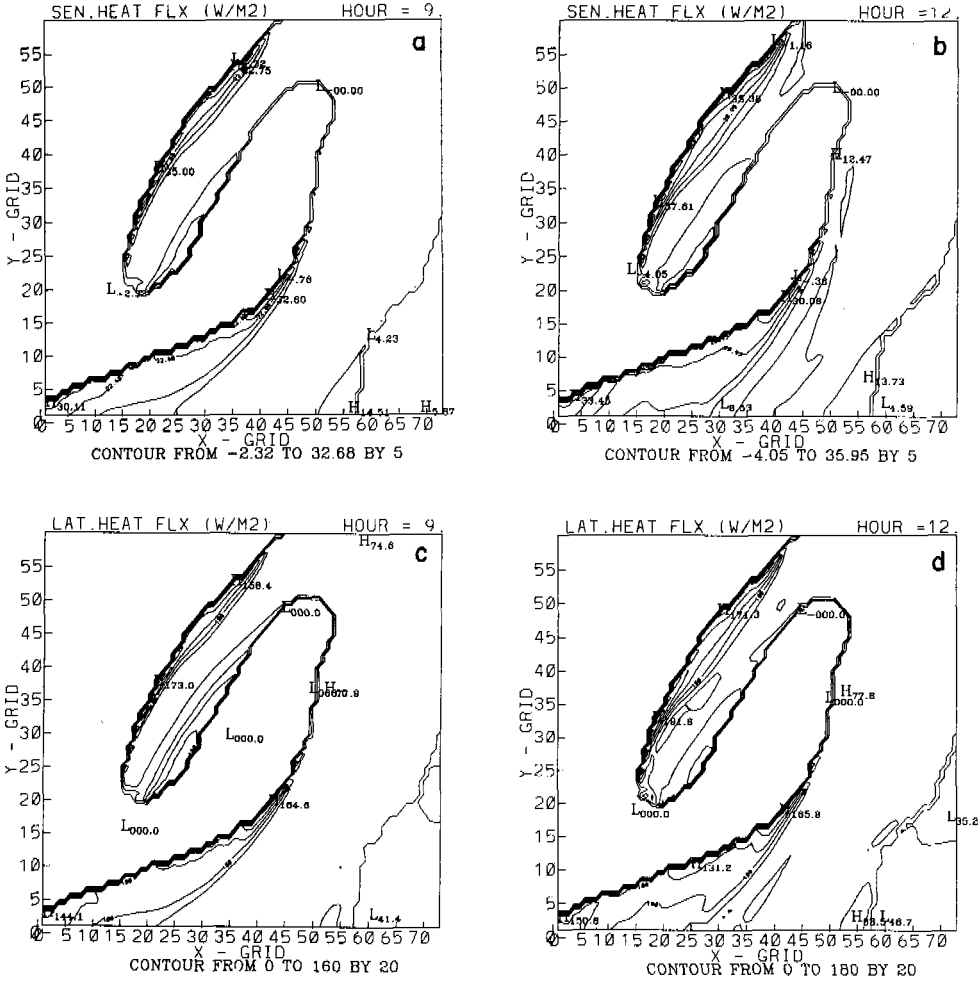

Figure 8
Surface sensible heat fluxes in Wm^{-2} at (a) 9 h and (b) 12 h and surface latent heat fluxes in Wm^{-2} at (c) 9 h and (d) 12 h of model simulation for case C1.

The vertical variation of TKE (Fig. 9) indicates a boundary layer depth of about 1.8 km over the filament and 1.5 km over the Gulf Stream. The mesoscale circulation extends to about 1.5 km (Fig. 9d). In early stages (not shown), a low level jet (LLJ) forms over the Gulf Stream filament with a maximum wind speed of 4.7 m s^{-1} at a height of about 400 m from the surface. This LLJ remains in the same location after 9 h of model simulation with a maximum wind speed of 6.3 m s^{-1} (Fig. 9c). At 12 h, the predicted boundary layer height remains the same (Figs. 10a and 10b). However, the maximum wind speed increases to 6.9 m s^{-1} (Figs. 10c and 10d). Observational analysis by REDDY and RAMAN (1994) for 10 February 1986 indicated a low level jet in the region of mesoscale circulation.

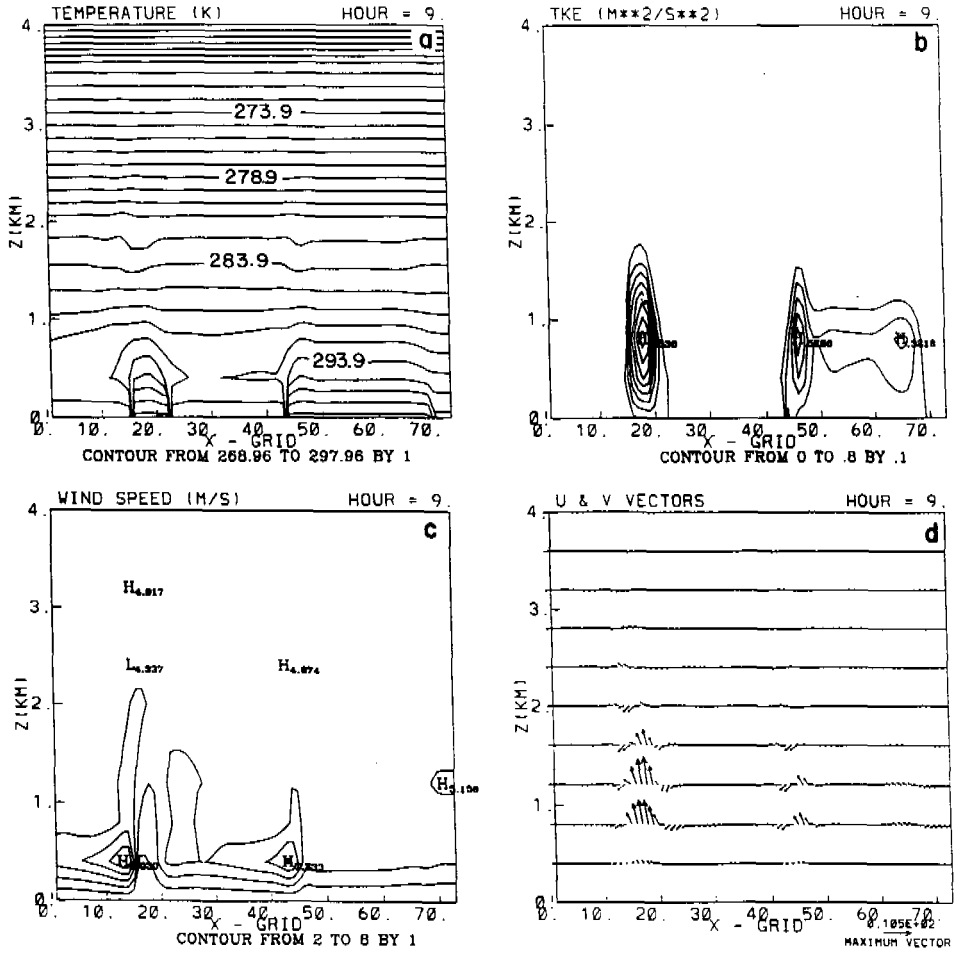

Figure 9
Vertical cross sections of (a) potential temperature θ (°C), (b) TKE ($m^2 s^{-2}$), (c) wind speed ($m s^{-1}$) and (d) U and W vectors ($m s^{-1}$) at 9 h of simulation for case C1. A maximum TKE of 0.85 $m^2 s^{-2}$ is predicted over the Gulf Stream filament (grid # 20).

Vertical cross sections of cloud water (q_c) and rainwater (q_r) are given in Figure 11. The contours of predicted cloud water show a good correlation between the development of the convergence zone and the formation of clouds, as one would expect. During the early stages (at 9 h, Fig. 11a), clouds begin to form along the edges of the filament. Clouds intensify with time over the filament and cover a wider area. However, there is no cloud or rainwater over the Gulf Stream (Figs. 10b and 10c). An intense rain band forms over the filament (Fig. 11d) after 12 h. The maximum model predicted cloud water and rainwater occur over the

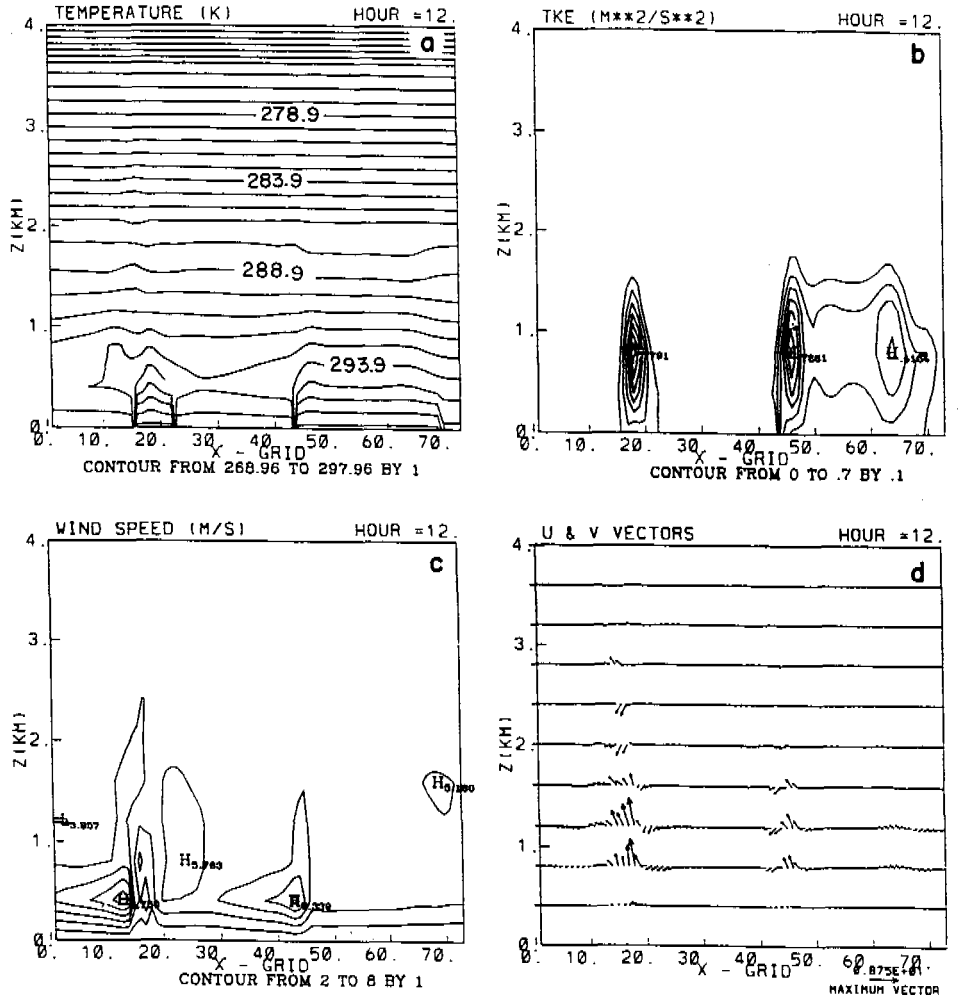

Figure 10
Vertical cross sections of (a) potential temperature θ (°C), (b) TKE ($m^2 s^{-2}$), (c) wind speed ($m s^{-1}$) and (d) U and W vectors ($m s^{-1}$) at 12 h of simulation for case C1. A maximum TKE of 0.99 $m^2 s^{-2}$ is predicted over the Gulf Stream filament (grid # 20).

filament and are about 6.6 g kg ^{1} and 0.6 g kg^{-1} respectively after 15 h of integration. These regions of maximum cloud water are in the regions of strong convergence.

In summary, the model results from case C1 compare well with the observational analysis (Fig. 2). The simulated flow between 12 h and 15 h is in good agreement with the observations on 10 February, 1986.

(b) Weak Ambient Wind (Case C2, wind speed of 0.1 $m s^{-1}$)

In order to investigate the influence of weak ambient winds on the mesoscale circulation, case C2 is conducted. A weak ambient wind of $U = 0.1 m s^{-1}$ and

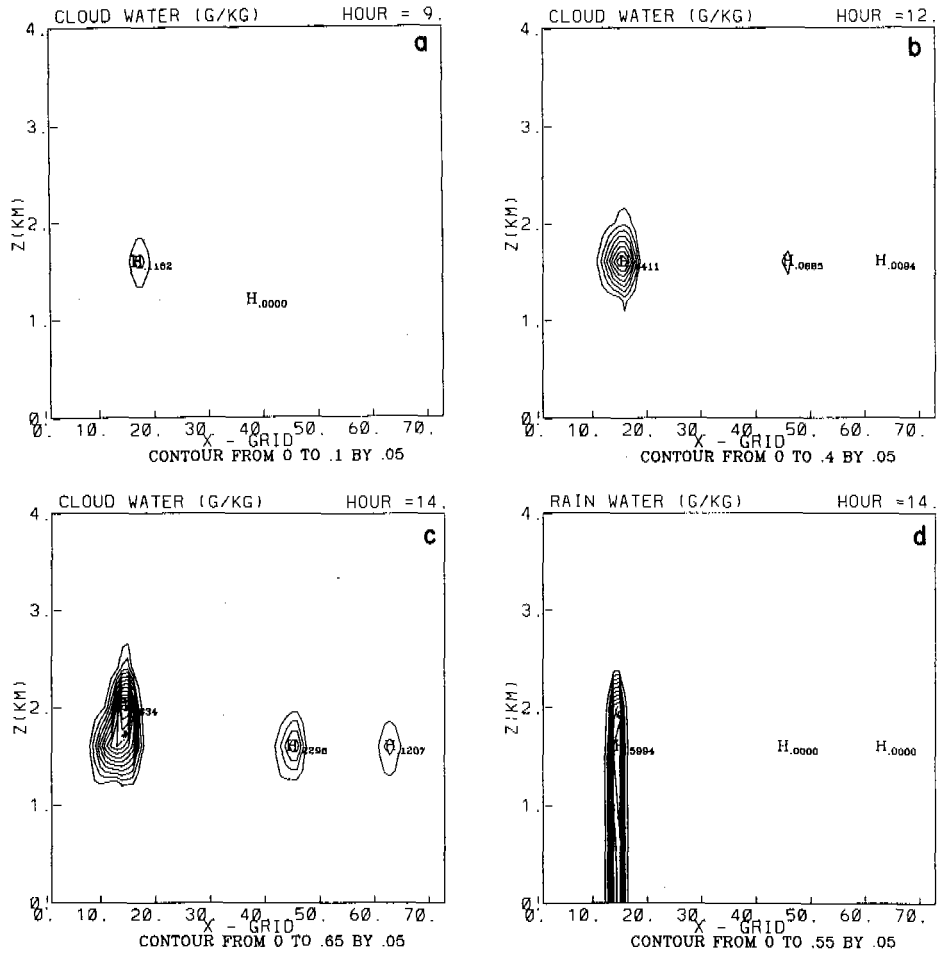

Figure 11
Vertical cross sections of cloud water (g kg $^{-1}$) at (a) 9 h, (b) 12 h, (c) 15 h and (d) rainwater at 15 h of model simulation for case C1.

$V = 0.1$ m s^{-1} is used as the initial condition. This case (C2) is similar to C1 except for the weak ambient wind.

The spatial distribution of U-V contours of horizontal divergence for case C2 after 9 h and 12 h simulation at $z = 50$ m are shown in Figure 12. A strong convergence zone forms along the maximum SST gradient (25°C, see Fig. 4a) with a cyclonic wind shift at the edges of the filament. When compared to case C1 (Fig. 5), convergence is much stronger over the filament with a weak convergence over the western edge of the Gulf Stream. The predicted maximum horizontal divergences for the case C2 are over the filament and the values after 9 h and 12 h of integration are about -7.72×10^{-5} s^{-1} and -9.91×10^{-5} s^{-1}, respectively. These

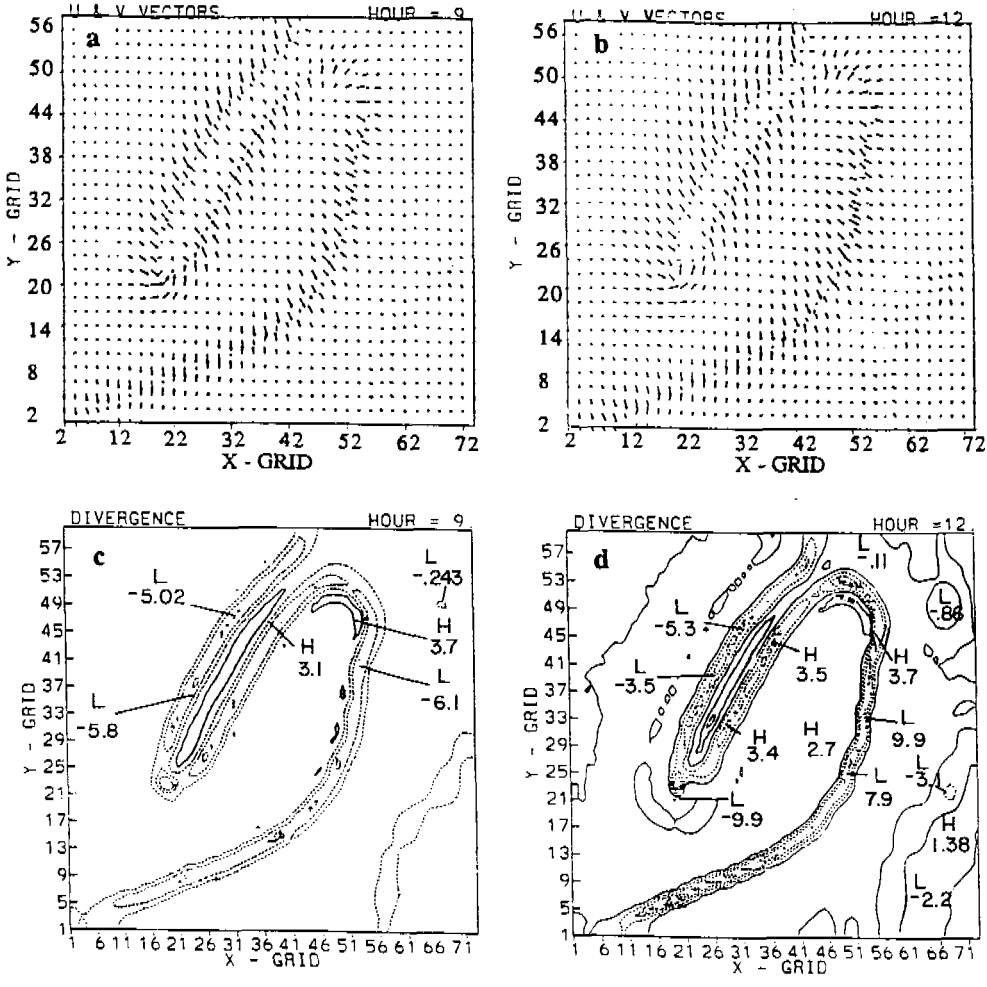

Figure 12
Spatial distribution of U and V vectors at (a) 9 h and (b) 12 h and horizontal divergence at (c) 9 h and (d) 12 h of model simulation for case C2 at 50 m height. The maximum wind speeds are 3 m s^{-1} and 3.9 m s^{-1} at 9 h and 12 h.

values are slightly higher than those predicted in case C1 (Fig. 6). For weak wind conditions, since there is no opposing flow over the Gulf Stream, convergence develops and intensifies quicker. Thus winds start converging considerably earlier (2 h of integration) for case C2 as compared to case C1 (6 h of integration).

After 15 h of model simulation (not shown), the low-level convergence along the western edge of the Gulf Stream decreases. However the circulation over the Gulf Stream filament intensifies further. Winds are accelerated towards the convergence zone with a wind speed of 4.6 m s^{-1}, considerably stronger than the ambient wind speed of 0.1 m s^{-1}. Using a mesoscale model, WARNER *et al.* (1990) found that in

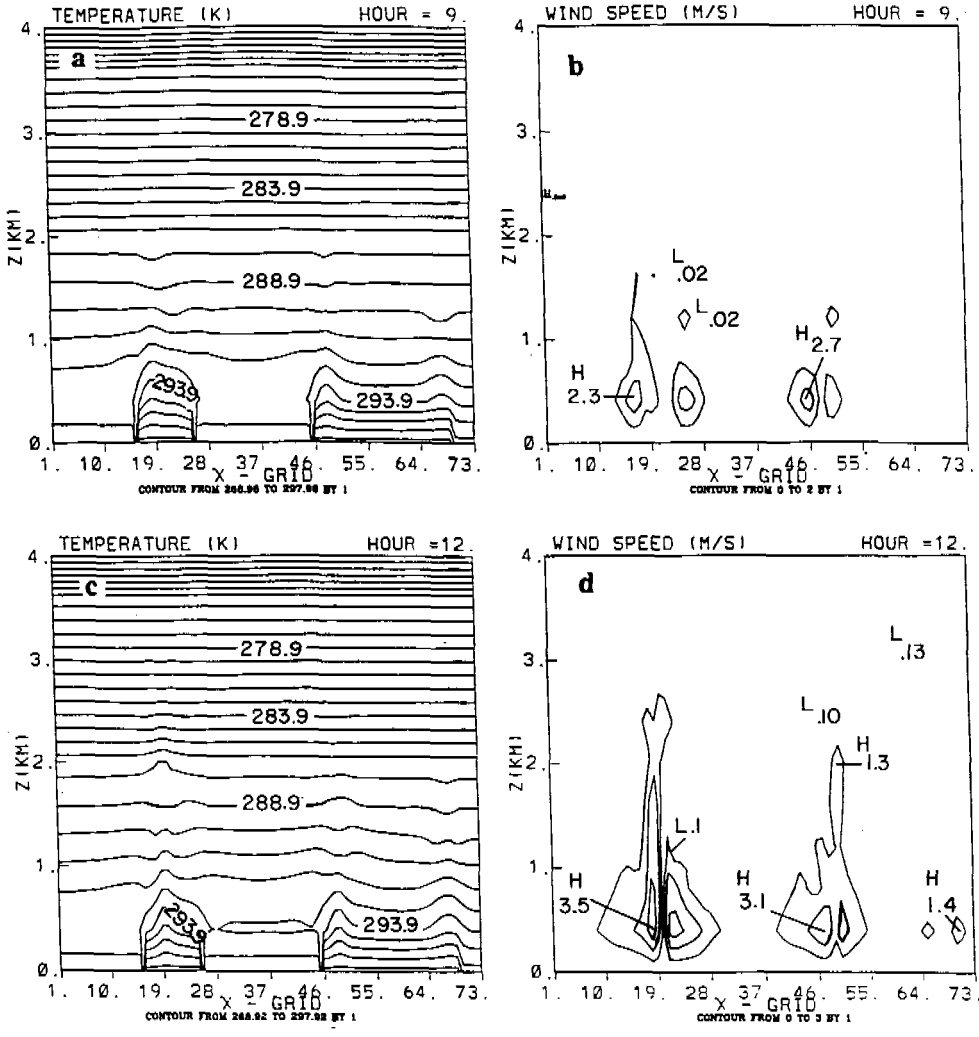

Figure 13
Vertical cross sections of potential temperature θ (°C) at (a) 9 h and (b) 12 h and wind speed (m s^{-1}) at (c) 9 h and (d) 12 h of integration for case C2.

weak wind conditions and with a large air-sea temperature difference of about 10°C, a maximum wind of 7.4 m s^{-1} can be produced in the marine boundary layer convergence zone.

Vertical cross sections of wind speed and potential temperature at 9 h and 12 h of model integration are illustrated in Figure 13. The θ contours show a well-defined sea breeze type of circulation extending to a height of about 300 m. The contours of wind speeds show a LLJ at a height of 300 m with a maximum wind speed of 3.3 m s^{-1}. Clouds develop after 9 h of integration over the filament (not

shown), but not over the Gulf Stream. However, after 12 h of model simulation, shallow clouds do develop over the Gulf Stream. The maximum cloud water at this hour over the Gulf Stream and the filament is 4.0 g kg^{-1} and 5.9 g kg^{-1}, respectively. A rainband with a maximum rainwater of 0.56 g kg^{-1} forms over the filament. No rainwater was predicted over the Gulf Stream.

The contours of sensible and latent heat fluxes (not shown) indicate a maximum total heat flux (SH + LH) of 190 Wm^{-2} after 12 h of model simulation. As expected, the predicted maximum total heat fluxes are in the region of maximum convergence (southern tip of the filament). For case C1, with an initial ambient wind speed of 3.5 m s^{-1}, the total heat flux predicted was 250 Wm^{-2} at the same model hour.

The results of these two cases, C1 (moderate winds) and C2 (weak winds) are quite different. Though convergence develops quickly and quite earlier in weak winds as compared to moderate winds along the maximum SST gradients, they are too weak to develop a mesoscale circulation over the filament. Again, because of the weak convergence predicted by the model, no cloud or rain developed over the Gulf Stream or the filament.

5.2 Simulation Without the Filament

Case C3 is conducted to investigate the influence of the Gulf Stream filament on the formation of the mesoscale circulation. This case (C3) is the same as case C1, except that the Gulf Stream filament is absent. An initial ambient wind speed of 3.5 m s^{-1} is used.

Vectors indicating the predicted horizontal winds and contours of horizontal divergence at 50 m height after 12 h and 15 h of model simulation for the case without the filament (case C3) are shown in Figure 14. At 9 h (not shown), a weak convergence zone forms along the western edge of the Gulf Stream with a maximum divergence of -0.9×10^{-5} s^{-1}. Winds increase moderately towards the Gulf Stream with a maximum wind speed of 4.3 m s^{-1} over the core of the Gulf Stream. Increase in wind speed and the horizontal convergence are thus minimal. Model predicted a maximum ascent of 0.25 cm s^{-1} after 15 h of simulation, as opposed to 11.5 cm s^{-1} for case C1 (with the filament) for the same location. The model results in this case (without the filament) do not show cyclonic turning of wind flow predicted for the case with the filament. It is believed that the curvature in SST gradients caused by the filament is important for the occurrence of closed circulation. The contours of predicted sensible and latent heat fluxes are shown in Figure 15. These predicted total heat fluxes are about 70 Wm^{-2} in case C3 (Figs. 15a,c) as compared to 200 Wm^{-2} in case C1 (Figs. 8a,c) after 9 h of model simulation. There was very little increase in these total heat fluxes (by about 10 Wm^{-2}) after 15 h of simulation in case C3 (Figs.

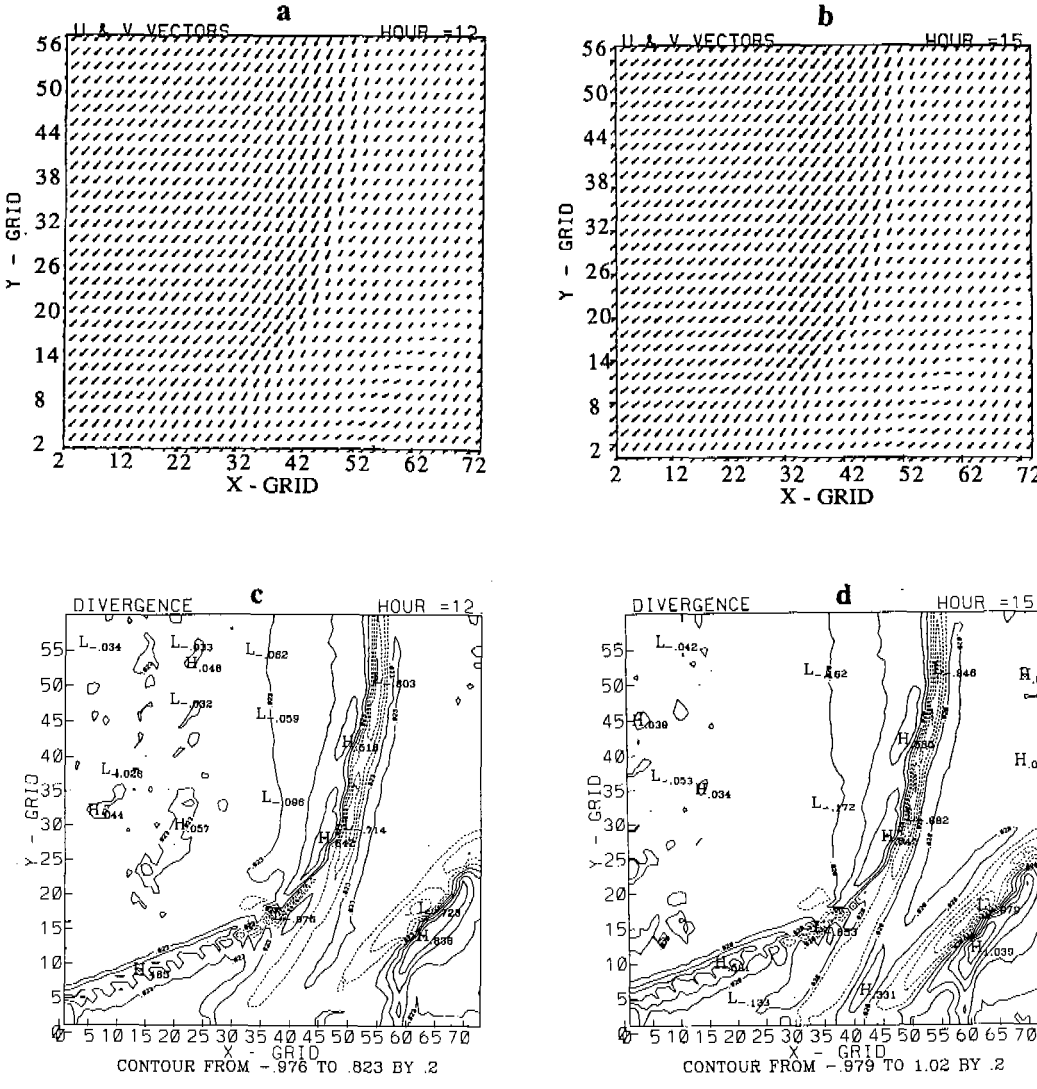

Figure 14

Spatial distribution of U and V at (a) 12 h and (b) 15 h and horizontal divergence at (c) 12 h and (d) 15 h of model simulation for case C3 at 50 m height. The maximum wind speeds are 3 m s $^{-1}$ and 3.9 m s^{-1} at 9 h and 12 h, respectively.

15b,d). These small values of total heat fluxes for the case without the filament are due to a relatively small increase in the wind speed. The weak convergence zone which existed until 15 h dissipated later on. Clouds did not develop in this simulation.

Figure 16 shows the vertical cross sections of wind speed and potential temperature after 9 h and 12 h of model simulations. The vertical cross section of the wind

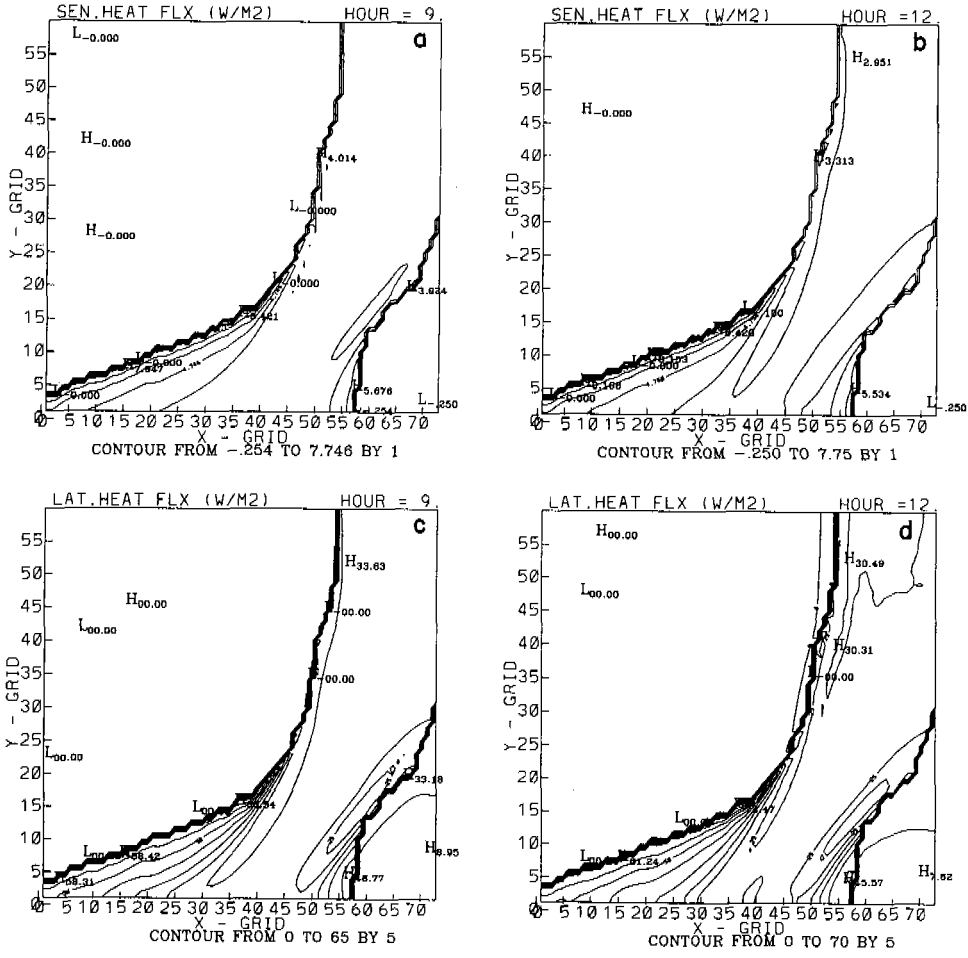

Figure 15
Surface sensible heat fluxes in Wm^{-2} at (a) 9 h and (b) 12 h and surface latent heat fluxes in Wm^{-2} at (c) 9 h and (d) 12 h of model simulation for case C3.

speed indicates a low-level jet near the western edge of the Gulf Stream with maximum magnitudes of 4.1 m s $^{-1}$ and 4.9 m s^{-1} after 9 h and 12 h of integration, respectively. Potential temperature contours show an increase in boundary layer depth from 400 m to 700 m towards the warmer waters.

In summary, the predicted values of variables (U, V, W and q_c) for the case without the filament (case C3) are considerably less than that with the filament (case C1), apparently because of the lack of strong convergence and convection that existed in case C1 due to the developing mesolow over the filament.

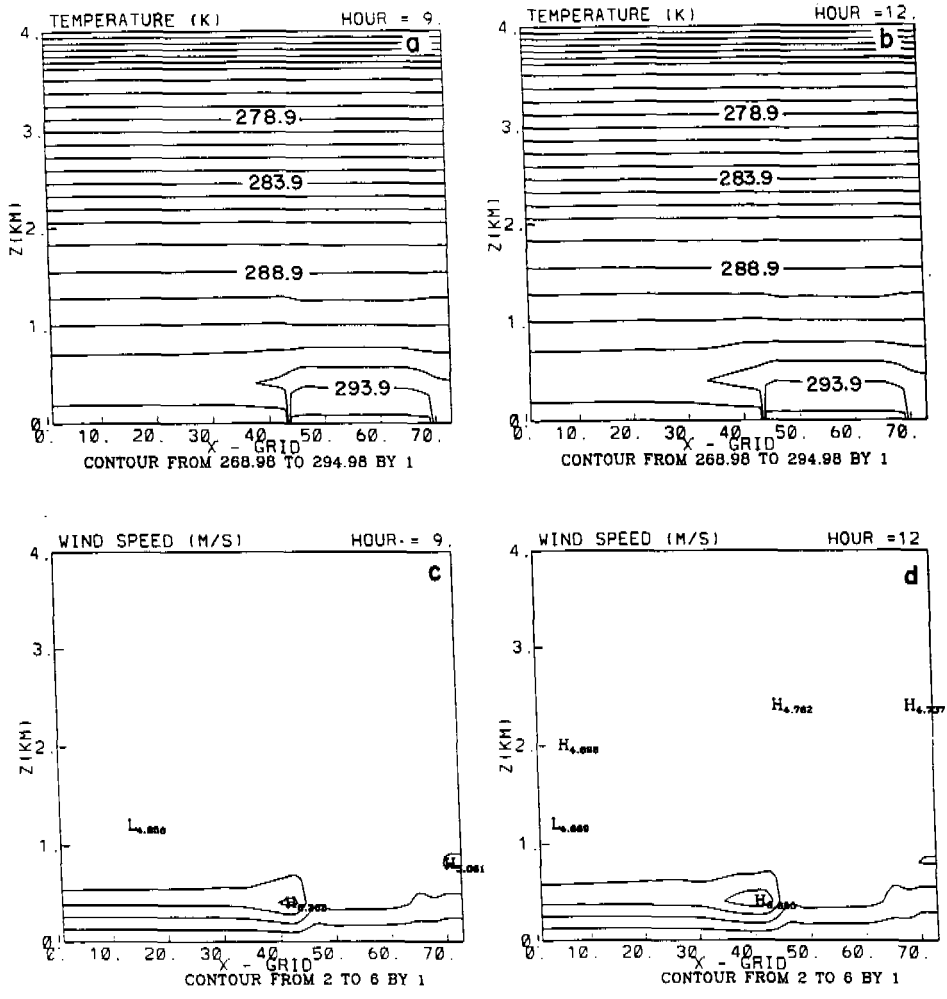

Figure 16
Vertical cross sections of potential temperature θ (°C) at (a) 9 h and (b) 12 h and wind speed (m s^{-1}) at (c) 9 h and (d) 12 h of integration for Case C3.

5.3 Simulation with Observed SSTs

It will be of interest to investigate the effect of observed SST distribution (Fig. 4b) and compare the results against the control experiment with constant SSTs west of the filament (Fig. 4a). For this purpose, case C4 is conducted with observed SST distribution in the vicinity of the Gulf Stream filament. This experiment is similar to the control run (C1) except for the SST distribution.

Figure 17 illustrates the U and V vectors and contours of pressure at 50 m height. The spatial distribution of U and V are similar to that predicted for case C1

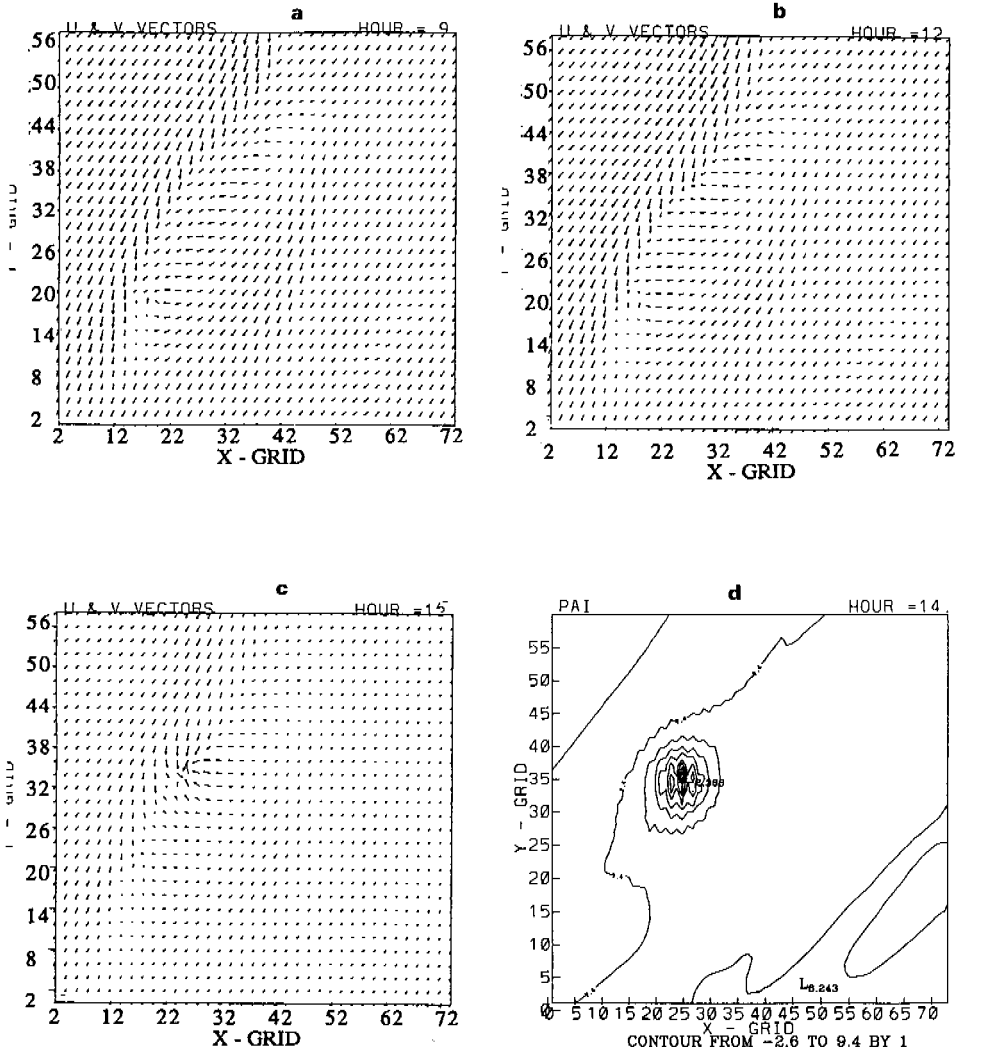

Figure 17
Spatial distribution of U and V vectors at (a) 9 h, (b) 12 h, (c) 15 h and (d) surface pressures (mb) after 15 h of model simulation for case C4 at 50 m height. The maximum wind speeds are 5.0 m s^{-1}, 8.1 m s^{-1} and 11.3 m s^{-1} at 9 h, 12 h and 15 h, respectively.

with the maximum convergence along the edges of the filament. As can be seen from Figures 17a, 17b and 17c, a mesolow develops after 6 h of model integration and intensifies into a cyclone over the Gulf Stream filament after 15 h of simulation (Fig. 17d). The observational analysis on 11 February at 1200 UTC (not shown) indicates the deepening of the surface mesolow into a mid-latitude cyclone. When a mesolow forms due to low-level forcing and is in phase with an upper level

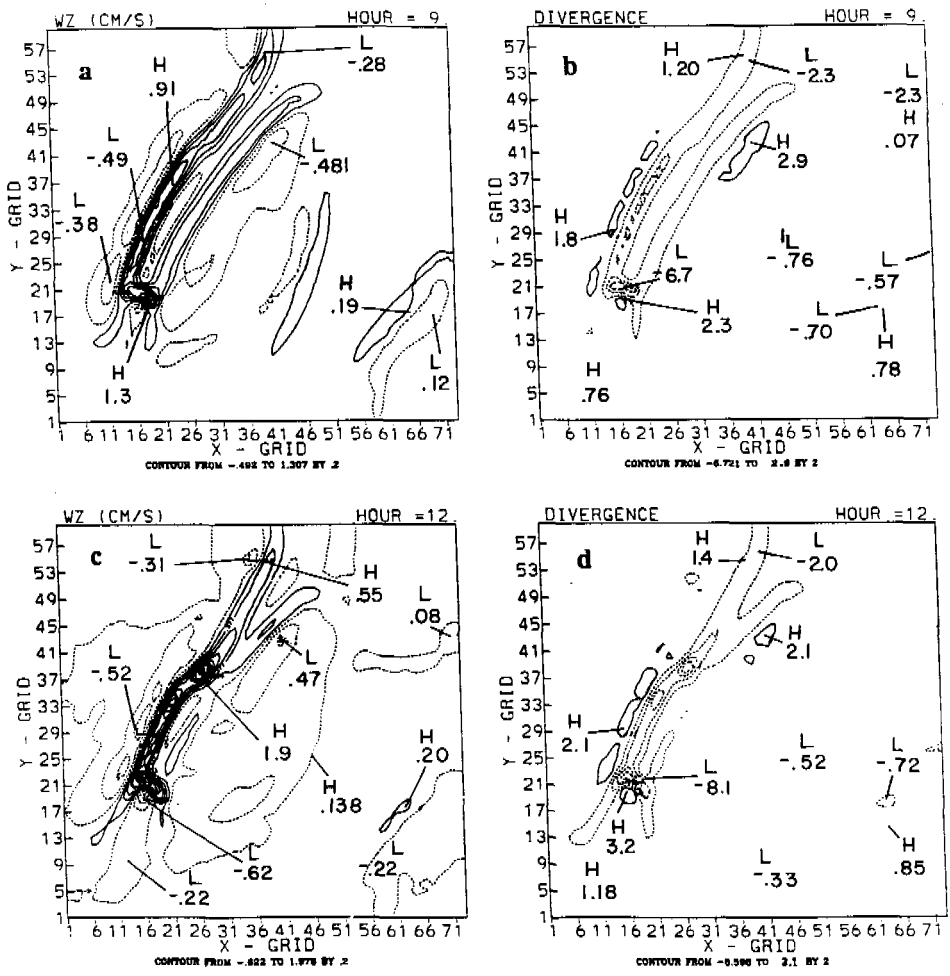

Figure 18
Spatial distribution of (a) vertical velocity in cm s $^{-1}$ at 9 h, (b) horizontal divergence ($\times 10^{-5}$) at 9 h, (c) vertical velocity in cm s^{-1} at 12 h, (d) horizontal divergence ($\times 10^{-5}$) at 12 h of model simulation at 50 m height for case C4.

disturbance, cyclogenesis could result (UCCELLINI *et al.*, 1986). The 500 mb analysis on 11 February indicated a mid-tropospheric trough over the eastern United States coastline.

The contours of vertical velocities and horizontal divergences (Fig. 18) once again indicate that the maximum convergence is near the filament. The maximum model predicted convergence ($-6.7 \times 10^{-5}\ s^{-1}$) is close to the observed value ($-7.1 \times 10^{-5}\ s^{-1}$). The contours of sensible and latent heat fluxes (Fig. 19) indicate sharp gradients along the edges of the filament. However, the model predicted total heat fluxes (205 Wm^{-2}) are somewhat less than those observed (240 Wm^{-2}) in this region.

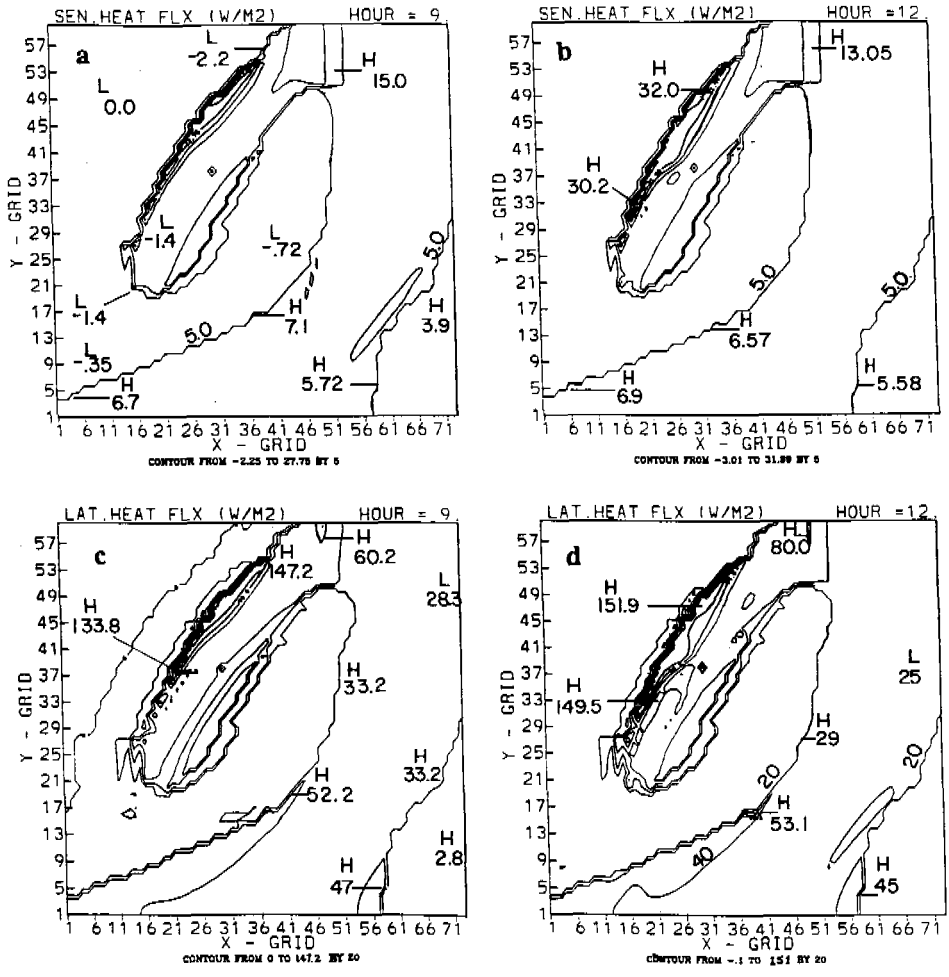

Figure 19
Surface sensible heat fluxes in Wm^{-2} at (a) 9 h and (b) 12 h and surface latent heat fluxes in Wm^{-2} at (c) 9 h and (d) 12 h for case C4.

Figure 20 shows the cross sections of U and V vectors and wind speeds after 9 h and 12 h of model simulation. As expected, the U and V vectors indicate a sea-breeze type of circulation near the Gulf Stream filament. The results from the cross sections of wind distribution (Figs. 20a and 20c) indicate the existence of a low-level jet with a maximum speed of 7.3 m s^{-1} at an altitude of 400 m. In the observational study (REDDY and RAMAN, 1994), the LLJ was observed at a height of about 400 m from the surface. The cross section of potential temperature and TKE (Fig. 21) shows a boundary layer height extending to 1500 m. This compares well with the observed height of 1100 m.

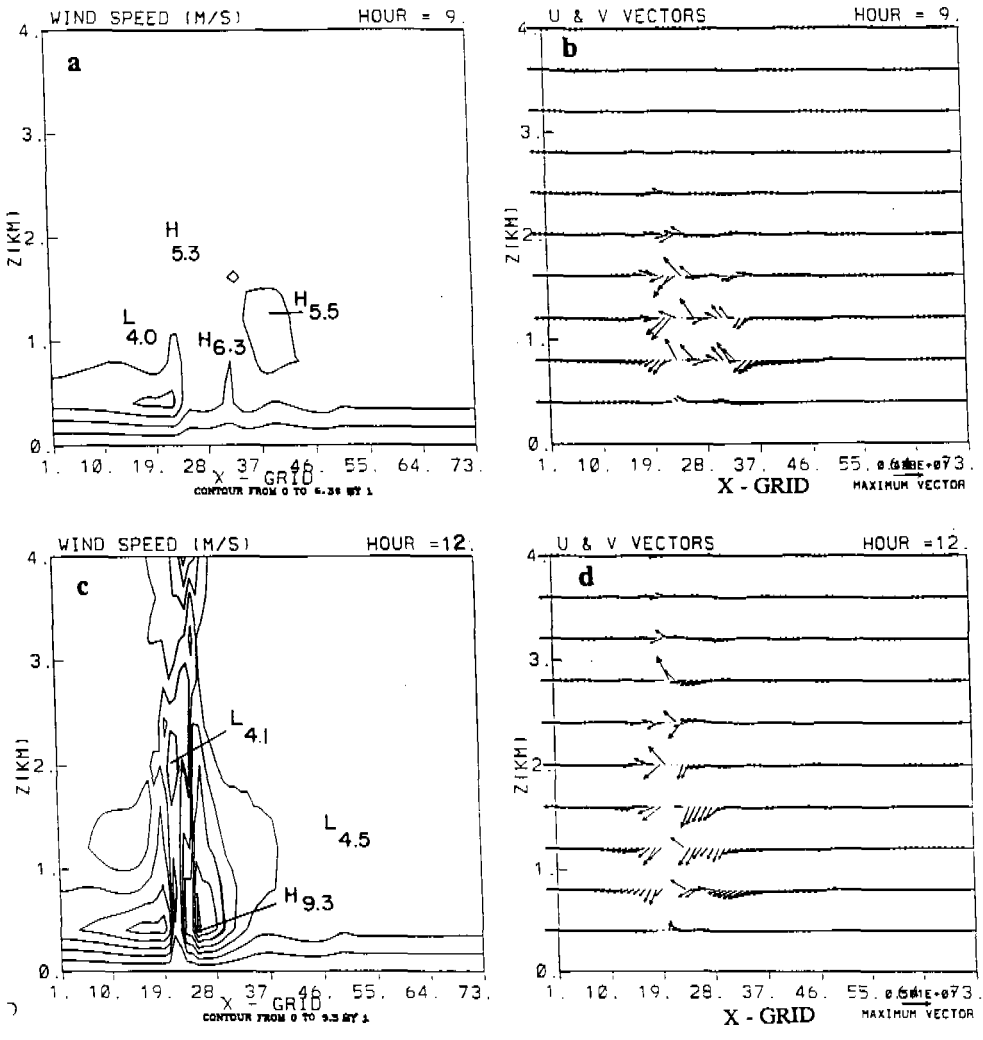

Figure 20
Vertical cross sections of wind speed (m s^{-1}) at (a) 9 h and (b) 12 h and U and W vectors at (c) 9 h and (d) 12 h of integration for case C4.

A comparison of model results of case C4 (realistic SST, see Fig. 4b) with case C1 (constant SST of 18 C west of the filament, see Fig. 4a) with the same initial conditions indicates similar results. However, the mesoscale circulation and convection develop earlier along the filament in case C1 as compared to case C4. Earlier development is probably caused by the sharp increase in the SST gradient in case C1 as compared to a gradual increase in case C4. In summary, the model results from both C1 and C4 compare well with the observations with small differences in the extent and the intensification of the circulation. Both the cases (C1 and C4)

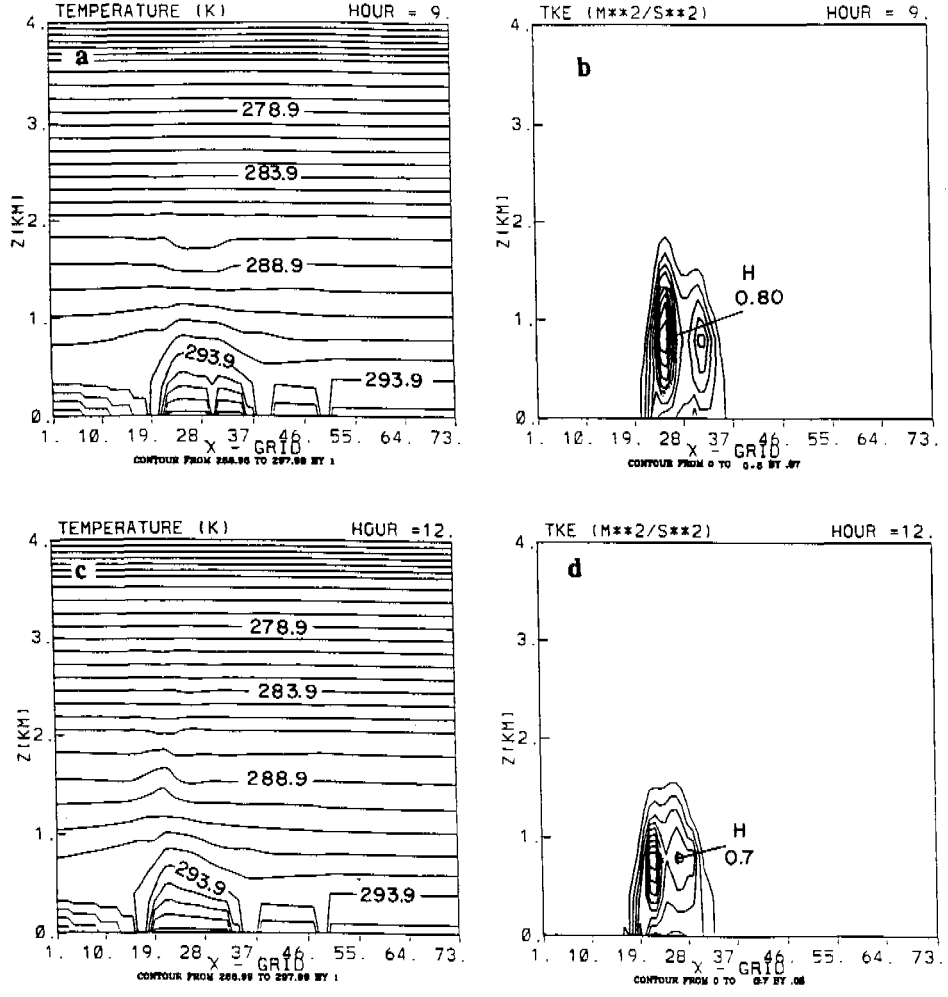

Figure 21
Vertical cross sections of potential temperature θ (°C) at (a) 9 h and (b) 12 h and TKE ($m^2 s^{-2}$) at (c) 9 h and (d) 12 h of model integration for case C4.

simulated offshore mesoscale circulation and the low-level jet at a height comparable with the observations. A comparison of numerical model results after 12 h of simulation to observations over a Gulf Stream filament is given in Table 3.

6. *Conclusions*

A mesoscale numerical model is used to investigate circulations over a Gulf Stream filament. Several sensitivity tests are carried out to isolate the effect of the

Table 3

Comparison of 12 h model predictions with observations over the Gulf Stream filament

Case	Wind speed ($m\ s^{-1}$)	Vertical velocity ($cm\ s^{-1}$)	Horizontal convergence ($\times 10^{-5}\ s^{-1}$)	Total heat flux (Wm^{-2})
C1	11.8	11.5	7.1	250
C2	4.6	6.8	9.9	190
C3	4.9	0.3	0.9	75
C4	7.3	2.5	6.7	205
OBS	12.0	–	7.1	240

ambient wind and the presence of the filament. Results indicate the development of a mesolow circulation over the Gulf Stream filament. The convergence zone over the filament is stronger as compared to the one along the western edge of the Gulf Stream. The predicted values of total heat flux and the horizontal convergence are close to the observations. Large values of cloud water and rainwater are predicted over the filament.

When the model simulation is performed without the Gulf Stream filament, the mesolow did not form. Also, horizontal convergence is much weaker. Domain maximum values of the sensible and latent heat fluxes for Case C3 (without the filament) are about one fourth of the values for Case C1 (with the filament). It appears that the curvature in the SST gradients caused by the filament and the shape of the filament are important for the occurrence of a closed circulation leading to the development of a mesolow.

Acknowledgements

This study was supported by the Division of Atmospheric Sciences, National Science Foundation under grant ATM-92-12636 and by the Department of Energy under contract 091575-A-Q1 with Pacific Northwest Laboratories. Computer resources were provided by the North Carolina Supercomputing Center, Research Triangle Park, NC.

References

ATLAS, D., CHOU, S.-H., and BYERLY, W. P. (1983), *The Influence of Coastal Shape on Winter Mesoscale Air-sea Interaction*, Mon. Wea. Rev. *111*, 245–252.

BROST, R. A. (1976), *Air Mass Modification in the Atmosphere's Boundary Layers: A Study Using a Two-dimensional Numerical Model with a Higher Order Turbulence Closure*, Ph.D. Thesis, submitted to the Department of Meteorology, University of Wisconsin, Madison.

BUSINGER, J. A., WYNGAARD, J. C., IZUMI, Y., and BRADLEY, E. F. (1971), *Flux-profile Relationships in the Atmospheric Surface Layer*, J. Atmos. Sci. *28*, 181 189.

CIONE, J. J., RAMAN, S., and PIETRAFESA, L. J. (1993), *The Importance of Low-level Processes on Offshore Cyclonic Intensification for two U.S. East Coast Storms*, Mon. Wea. Rev. *121*, 421 430.

HOLT, T. R., and RAMAN, S. (1990), *Marine Boundary Layer Structure and Circulation in the Region of Offshore Redevelopment of a Cyclone during GALE*, Mon. Wea. Rev. *118*, 392–410.

HUANG, C. Y., and RAMAN, S. (1988), *A Numerical Modeling Study of the Marine Boundary Layer over the Gulf Stream During Cold Air Advection*, Bound.-Layer Meteor. *45*, 251–290.

HUANG, C. Y., and RAMAN, S. (1990), *Numerical Simulations of Cold Air Advection over the Appalachian Mountains and the Gulf Stream*, Mon. Wea. Rev. *118*, 343 362.

HUANG, C. Y., and RAMAN, S. (1991), *A Three-dimensional Numerical Investigation of Carolina Coastal Front and the Gulf Stream Rainband*, J. Atmos. Sci. *49*, 560 584.

HUANG, C. Y., and RAMAN, S. (1992), *A Three-dimensional Numerical Investigation of a Carolina Coastal Front and the Gulf Stream Rainband*, J. Atmos. Sci. *49*, 560–584.

KLEMP, J. B., and DURRAN, D. R. (1983), *An Upper Boundary Condition Permitting Internal Gravity Wave Radiation in Numerical Mesoscale Model*, Mon. Wea. Rev. *111*, 430–444.

KUO, H. L. (1974), *Further Studies of the Parameterization of the Influence of Cumulus Convection on Large-scale Flow*, J. Atmos. Sci. *31*, 1232–1240.

MAHRER, Y., and PIELKE, R. A. (1977), *The Effects of Topography on the Sea and Land Breeze in a Two-dimensional Model*, Mon. Wea. Rev. *105*, 1151–1162.

MAHRER, Y., and PIELKE, R. A. (1978), *A Test of an Upstream Spline Interpolation Technique for the Advection Terms in a Numerical Mesoscale Model*, Mon. Wea. Rev. *106*, 818–830.

MELLOR, G. L., and YAMADA, T. (1982), *Development of a Turbulence Closure Model for Geophysical Fluid Problems*, Rev. Geophys. Space Phys. *20*, 851 875.

MILLER, M. J., and THORPE, A. J. (1981), *Radiation Conditions for the Lateral Boundaries of Limited Area Numerical Models*, Q. J. R. Meteor. Soc. *107*, 615–628.

MOENG, C.-H., and ARAKAWA, A. (1980), *A Numerical Study of a Marine Subtropical Stratus Cloud Layer and its Stability*, J. Atmos. Sci. *37*, 2661–2676.

PETTERSSEN, S. (1956), *A Contribution to the Theory of Frontogenesis*, Geofys. Publ. *11*, 1 27.

PIETRAFESA, L. J. (1978), *On Continental Margin Processes in the South Atlantic Bight*, Trans. Am. Geophys. Union *60*, 218 281.

PIETRAFESA, L. J. (1983), *Survey of a Gulf Stream Frontal Filaments*, Geophys. Res. Lett. *10* (3), 203–206.

RAMAN, S., and RIORDAN, A. J. (1988), *The Genesis of Atlantic Lows Experiment: The Planetary Boundary-layer Subprogram of GALE*, Bull. Am. Meteor. Soc. *69*, 161–172.

REDDY, N. C., and RAMAN, S. (1994), *Observations of a Mesoscale Circulation over the Gulf Stream Region*, The Global Atmos. and Ocean System *2*, 21 39.

ROONEY, D. M., JANOWITZ, G. S., and PIETRAFESA, L. J. (1978), *A Simple Model of Deflection of the Gulf Stream by the Charleston Rise*, Gulf Stream *11*, 1 7.

SANDERS, F., and GYAKUM, J. R. (1980), *Synoptic-dynamic Climatology of the Bomb*, Mon. Wea. Rev. *108*, 1589–1606.

UCCELLINI, L. W., BRILL, K. F., PETERSEN, R. A., KEYSER, D., AUNE, R., KOCIN, P.J., and JARDIN, M. des (1986), *A Report of the Upper Level Wind Conditions Preceding and During the Shuttle Challenger (STS 51L) Explosion*, Bull. Am. Meteor. Soc. *67*, 1248 1265.

VON ARX, W. S., BUMPUS, D. F., and RICHARDSON, W. S. (1955), *On the Fine Structure of the Gulf Stream Front*, Deep-Sea Research *3* (1), 46–55.

WAI, M. M. (1988), *Modeling the Effects of the Spatially Varying Sea-surface Temperature on the Marine Atmospheric Boundary Layer*, J. Appl. Meteor. *27*, 5–19.

WAI, M. M., and STAGE, S. A. (1989), *Dynamical Analyses of Marine Atmospheric Boundary Layer Structure near the Gulf Stream Oceanic Front*, Quart. J. Roy. Meteor. Soc. *115*, 29 44.

WARMING, R. F., KUTLER, P., and LOMAX, H. (1973), *Second- and Third-order Noncentered Difference Schemes for Nonlinear Hyperbolic Equations*, AIAA J. *11*, 189–196.

WARNER, T. T., LAKHTAKIA, M. N., and DOYLE, J. D. (1990), *Marine Atmospheric Boundary Layer Circulations Forced by Gulf Stream Sea-surface Temperature Gradients*, Mon. Wea. Rev. *118*, 309–323.

(Received July 20, 1995, accepted April 1, 1996)